Cryst. Res. Technol. **45**, No. 4, 414 – 420 (2010) / **DOI** 10.1002/crat.201000026

Structural, optical and photoconductive properties of electron beam evaporated CdS_xSe_{1-x} films

K. Sivaramamoorthy[1], S. Asath Bahadur[2], M. Kottaisamy[3], and K. R. Murali*[4]

1 Department of Physics, Rajapalayam Rajus' College, Rajapalayam, India
[2] Dept of Physics, Kalasalingam University,Krishnan Koil, India
[3] Dept of Chemistry, Kalasalingam University,Krishnan Koil, India
[4] Electrochemical Materials Science Division, CECRI, Karaikudi, India

Received 14 January 2010, revised 16 January 2010, accepted 19 January 2010
Published online 29 January 2010

Key words CdS_xSe_{1-x}, thin films, II – VI, semiconductors.

CdS_xSe_{1-x} films were deposited by the electron beam evaporation technique on glass substrates at different temperatures in the range 30 – 300 °C using the laboratory synthesized powders of different composition. The films exhibited hexagonal structure and the lattice parameters shifted from CdSe to CdS side as the composition changed from CdSe to CdS side. The bandgap of the films increased from 1.68 to 2.41 eV as the concentration of CdS increased. The root-mean-roughness (RMS) values are 3.4, 2.6, 1.2 and 0.6 nm as the composition of the films shifted towards CdS side. The conductivity varies from 30 Ωcm^{-1} to 480 Ωcm^{-1} as the 'x' value increases from 0 to 1. The films exhibited photosensitivity. The PL spectrum shifts towards lower energies with decreasing x, due to the decrease of the fundamental gap with Se composition.

1 Introduction

Group II–VI semiconductors with energy gaps covering the visible spectral range are promising candidates for opto-electronic devices [1,2]. CdS and CdSe are two very important wide gap semiconductors, because of their wide applications in optoelectronics, such as non-linear optics, visible-light emitting diodes and lasers [3]. However, for some opto-electronic applications it is important to be able to tune the emission wavelength. The tunability can be achieved through composition modulation, for example, alloyed II–VI semiconductor ternary of CdS_xSe_{1-x}, $Zn_xMg_{1-x}O$, and $Cd_{1-x}Mn_xS$ with continuously tuned band gap have been reported [4–8]. Consequently, wavelength tunable emission can be achieved from ternary compounds by simple adjustment of composition. The alloy of CdSSe should have more applications since its band gap can be tuned by means of the composition in between 2.44 eV (for CdS) and 1.72 eV (for CdSe), almost covering the entire visible range. However, for the efficient opto-electronic device application, material is usually between CdS in which very high sensitivity is possible but response time is high and CdSSe in which a lower response time is possible at the cost of some loss in sensitivity [9].

Considering the advantages of the ternary alloy CdS_xSe_{1-x} thin films, in this work, the ternary films were deposited by the electron beam evaporation technique using the laboratory synthesized CdS_xSe_{1-x} powders of different composition. The structural, compositional, morphological, optical and electrical properties and the results are discussed in the light of the literature available.

2 Experimental

CdS_xSe_{1-x} powders were prepared by the reaction of aqueous solutions of cadmium acetate, sodium seleno sulphate and thiourea under optimum conditions of pH ~10. This pH value was used to dissolve the $Cd(OH)_2$ formed by the addition of alkali to maintain a clear solution., obtained by the addition of ammonium

* Corresponding author: e-mail: muraliramkrish@gmail.com

hydroxide. 40 g of cadmium acetate was dissolved in 200 ml of triple distilled water, 25 g of thiourea was dissolved in 250 ml of triple distilled water by gentle heating, seleno sulphate solution was prepared by dissolving 30 g of selenium in a sodium sulphite solution (prepared by dissolving 235 g of sodium sulphite in 500 ml triple distilled water). The cadmium acetate solution was taken in a three litre flask fitted with grounded joints, and 150 ml of fresh ammonia was added when a clear solution of cadmium ammonia complex was obtained. To this clear solution different quantities of selenosulphate and thiourea solutions were taken in 100 ml of ammonia and added to the complex and refluxed on a heating mantle provided with facility for magnetically stirring the contents for two hours. 30 ml of ammonia was added at intervals of 30 min. The colour of the precipitate changed from orange colour to shiny bright black colour as the composition of the powder changed from sulphur rich to selenium rich side. The precipitate was kept for about 15 h and filtered through a Whatman 42 filter paper using Buchner funnel with vacuum suction arrangement. The powders were then washed with hot sodium sulphite to remove traces of selenium, and washed with hot acetic acid to remove traces of cadmium oxide. Further washing was continued until the pH of the filtrate was found to be neutral. Purified ethanol was employed for final washing to remove moisture. The powders were dried in vacuum oven. The powders were then annealed at 300 °C in argon atmosphere for 30 min to remove any traces of excess selenium. The powders were then stored in vacuum desiccators. The powders were checked for the purity by Atomic Absorption spectrometry (AAS). Table 1 shows the impurities present in the $CdS_{0.5}Se_{0.5}$ powders as a representative.

Table 1 AAS Analysis of the $CdS_{0.5}Se_{0.5}$ powders.

Sample	Impurity content in ppm							
	Cu	Fe	Ca	K	Na	Zn	Pb	Co
$CdS_{0.5}Se_{0.5}$ (prepared)	10	20	20	2	2	1	1	1

In the present work, a Hind Hivac Coating unit was used for electron beam evaporation. A vacuum of 10^{-6} Torr was maintained during evaporation. The source heater substrate distance was maintained as 20 cm. The laboratory synthesized powders of different composition were used as the source for electron beam evaporation. An operating voltage of 5 kV and 10 mA were used. The substrate temperature was varied in the range of 30 – 300 °C. Cleaned glass was used as the substrates for deposition of films. The substrate dimensions were 2 cm x 1 cm. After deposition of the films they were stored in desiccator before using them for characterization. Thickness of the films was in the range of 800 to 1200 nm with increase of Se composition. The films were characterized by Xpert PANalytical XRD unit. Optical measurements were made using Hitachi U3400 UV-Vis-NIR spectrophotometer. Surface morphological studies were made using molecular imaging systems AFM. The elemental composition was found using an energy-dispersive X-ray (EDX) spectrometer attached with the HITACHI Model S-3000H SEM instrument. PL studies were made at room temperature, using Varian Cary Eclipse Fluorescence Spectrophotometer. Photoconductivity and resistivity measurements were made by evaporating Indium on the edges of the films.

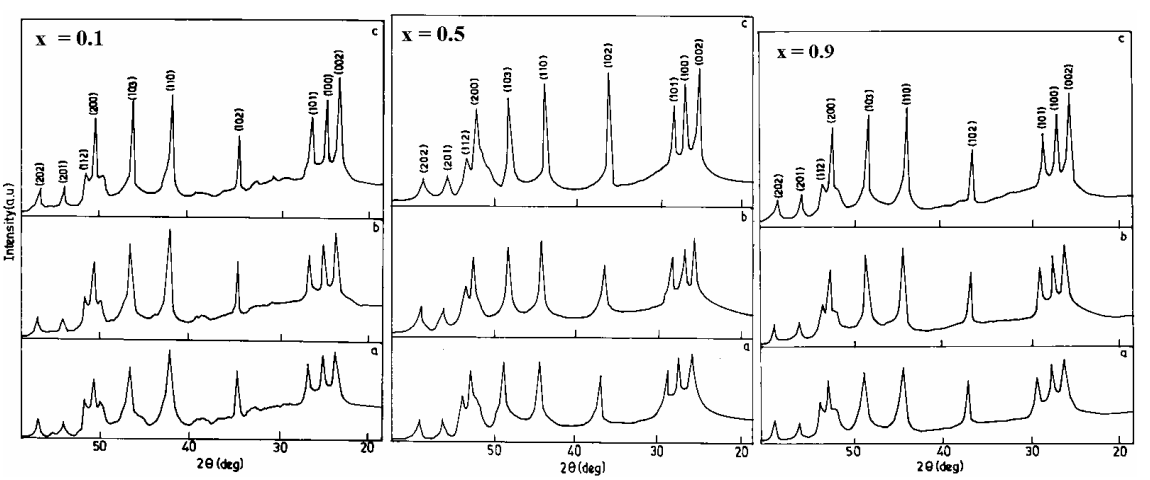

Fig. 1 XRD patterns of $CdS_{0.1}Se_{0.9}$ films of different composition deposited at different substrate temperatures (a) 50 °C (b) 150 °C (c) 300 °C.

3 Results and discussion

The XRD patterns of the films of different compositions obtained by using CuK_α radiation are shown in figure 1. The peaks corresponding to (100), (002), (101), (102), (110), (103) and (112) reflections were observed in all cases. The peaks were observed to shift to higher 2θ values as the 'x' value increased from 0 to 1. All the samples exhibited hexagonal structure and the lattice parameters 'a' and 'c' were calculated using the standard relation, $\frac{1}{d^2} = \frac{4}{3}\left[\frac{h^2 + hk + k^2}{a^2}\right] + \frac{l^2}{c^2}$. 'a' and 'c' values for CdSe and CdS are taken from the JCPDS data (JCPDS 6 – 314 for hexagonal CdS, JCPDS 8 – 459 for hexagonal CdSe). The variation of lattice constants of cadmium sulpho selenide films with composition is shown in figure 2. A linear variation of the lattice constants with composition indicates that Vegard's law is obeyed [10]. Similar variation has been observed for sintered pellets [11], flash evaporated layers [12], single crystals [13] and sprayed layers [14].

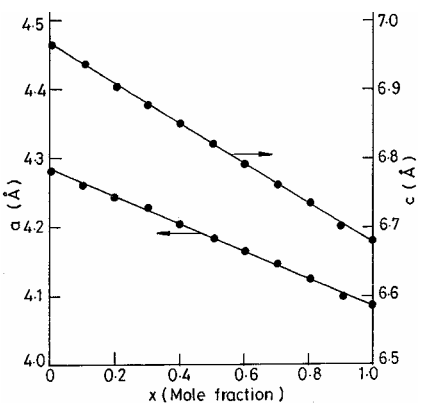

Fig. 2 Variation of lattice constants with increase of CdS mole fraction.

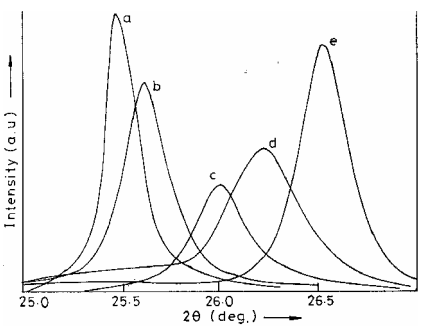

Fig. 3 Shift of the (002) peak with change of composition (a) x=0, (b) x=0.2, (c) x=0.4, (d) x=0.6, (e) x=1.0.

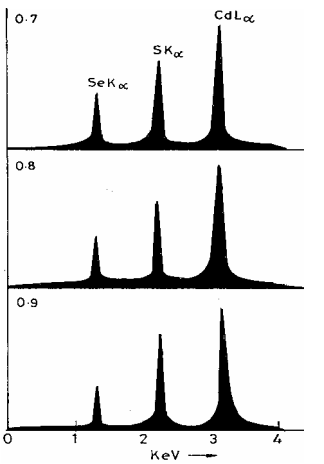

Fig. 4 EDAX spectrum of CdS_xSe_{1-x} films of different composition heat treated at 550 °C.

The c/a ratio in all the cases is around 1.634 which is in close agreement with the theoretical value obtained from the relation that the axial ratio in a regular hexagonal system is $2\sqrt{2}/\sqrt{3}$, that is 1.633 [15]. Figure 3 shows the shift of the (002) peak with composition. As the concentration of CdSe increases in the films the peak is observed to shift towards CdSe.

Table 2 Composition of CdS_xSe_{1-x} films.

Starting Composition	EDAX Analysis
$CdS_{0.9}Se_{0.1}$	$CdS_{0.89}Se_{0.11}$
$CdS_{0.8}Se_{0.2}$	$CdS_{0.80}Se_{0.20}$
$CdS_{0.7}Se_{0.3}$	$CdS_{0.70}Se_{0.30}$
$CdS_{0.6}Se_{0.4}$	$CdS_{0.58}Se_{0.42}$
$CdS_{0.5}Se_{0.5}$	$CdS_{0.49}Se_{0.51}$
$CdS_{0.4}Se_{0.6}$	$CdS_{0.39}Se_{0.61}$
$CdS_{0.3}Se_{0.7}$	$CdS_{0.28}Se_{0.72}$
$CdS_{0.2}Se_{0.8}$	$CdS_{0.19}Se_{0.81}$
$CdS_{0.1}Se_{0.9}$	$CdS_{0.09}Se_{0.91}$

Composition analysis was done by EDAX study and the composition of the powders is indicated in table 2. From the table, it is clear that the EDAX analysis data (Fig. 4) are almost similar to the theoretical composition expected from the starting materials. The data corresponding to CdLα, SeKα and SKα lines were used for estimating the composition.

The AFM images of the thin films of different compositon and deposited at different temperatures are shown in figure 5. The images were acquired in the constant friction mode scanning tips over a scanning area of 2 µm x 2 µm. The root-mean-roughness (RMS) values obtained from the figures are 3.4, 2.6, 1.2 and 0.6 nm, respectively. Obviously, the surface roughness decreased dramatically when the composition of the films shifted towards CdS side (x = 0.2 to x = 0.8).

Optical absorption measurements were made on the films of different composition deposited on glass substrates and annealed at 550 °C. The energy gap obtained by extrapolating the linear portion of the $(\alpha h\nu)^2$ vs hν plot to the energy axis yielded a direct band gap value of the film (Fig. 6). The band gap increases from 1.68 eV to 2.41 eV as the value of 'x' increases.

The electrical resistivity of the films was measured by the two probe technique. The influence of composition on the conductivity of the films is depicted in figure 7. The results on the films annealed at 550 °C are only presented, since they have exhibited maximum photoconductivity. The magnitude of the conductivity varies from 30 Ωcm^{-1} to 480 Ωcm^{-1} as the 'x' value increases from 0 to 1. The increase in conductance may be associated with increase in sulphur/selenium vacancies (due to decrease of depth of donor level associated with the sulphur/selenium vacancy) [16].

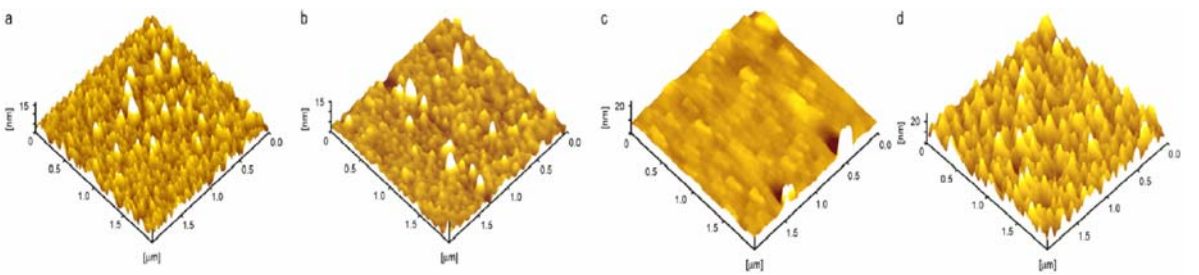

Fig. 5 Atomic force micrograph of the CdS_xSe_{1-x} films of different composition deposited at a different substrate temperatures (a) x = 0.2 (b) x = 0.4 (c) x = 0.6 (d) x = 0.8. (Online color at www.crt-journal.org)

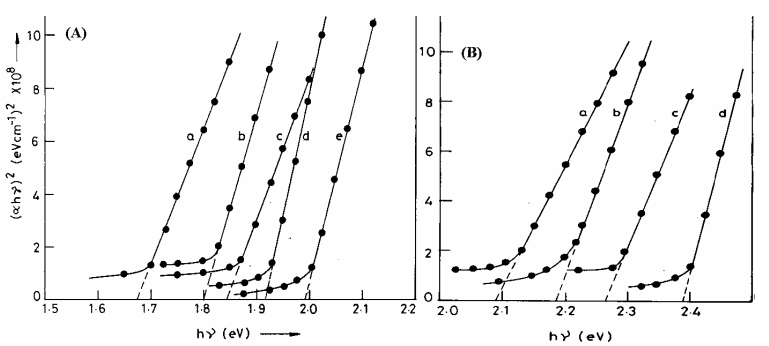

Fig. 6 $(\alpha h\nu)^2$ vs hν for the CdS_xSe_{1-x} films of different composition deposited at a substrate temperature of 300 °C (A) (a) x =0.1(b) x = 0.2 (c) x = 0.3 (d) x = 0.4 (e) x = 0.5 (B) (a) x = 0.6 (b) x = 0.7 (c) x = 0.8 (d) x = 0.9.

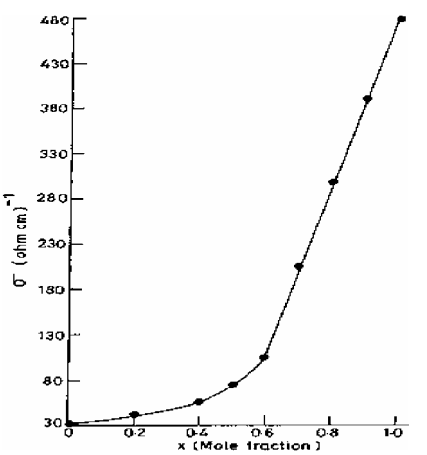

Fig. 7 Dependence of conductivity with composition for CdS_xSe_{1-x} films deposited at 300 °C.

In order to obtain very high photosensitivity, the post deposition heat treatment temperature was varied in the range of 500 – 600 °C. It was observed that temperature had a profound influence on the sensitivity and stability of the photoconductive cells. The photosensitivity of the films of different composition after heat treatment at 550 °C was studied and is shown in figure 8. As observed from the figure the films deposited at a substrate temperature of 300 °C have exhibited maximum photosensitivity, hence further studies were made only on the films deposited at a substrate temperature of 300 °C.

It is observed that as the post heat treatment temperature increases, the photosensitivity also increases. Higher temperatures lead to rapid decrease in light resistance. While at low temperature, instability of the cells is observed. Appropriate temperature is necessary to control the diffusion rates of impurities and mobile

defects so that optimum sensitivity and reasonable stability are obtained, besides useful light resistance. It is observed that a post deposition heat treatment temperature of 550 °C results in high photosensitivity as well as low light resistance.

Heat treatment time has a significant role to play in the process of obtaining useful photoconductive cells. As the time is gradually increased, significant lowering of light resistance is observed while practically no pronounced increase in dark resistance takes place. For 15 min post heat treatment, the dark resistance slightly increases while the light resistance attains a minimum. On further heating the samples, more sensitization centers get incorporated. The fall in light resistance with heat treatment duration, may also be attributed to the removal of grain boundaries due to optimum recrystallization

The variation of photocurrent with excitation intensity in cadmium sulphide type photoconductors is interesting and is of fundamental importance in the operation of these photoresistors in devices. As discussed earlier, the large photosensitivity associated with these materials arises due to the presence of compensated acceptors, which act as sensitizing centers. As the excitation intensity is increased at a fixed temperature, these centers become more active and photosensitivity sharply rises at some region of excitation. As the temperature is increased under a given excitation intensity, sensitivity is reported to fall [17].

Figure 9 depicts the variation of photocurrent with illumination at room temperature for CdS_xSe_{1-x} cells. An examination of the graphs reveals that as the selenide content is increased, the behaviour of the photocurrent with excitation intensity changes progressively towards the behaviour of cadmium selenide. Thus for cells with 'x' values less than 0.3, the super-linear behaviour is not observed under all experimental conditions. Further, the photocurrent at saturation decreases progressively as the selenide content is increased.

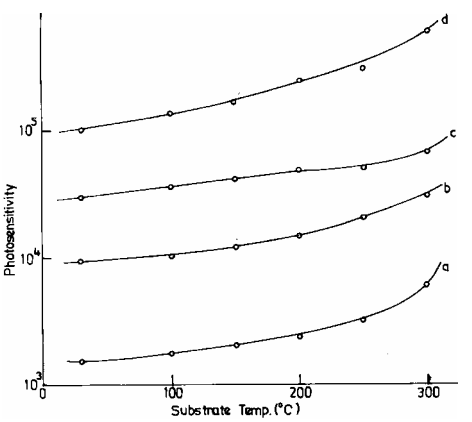

Fig. 8 Variation of photosensitivity of CdS_xSe_{1-x} films of different composition deposited at different substrate temperature after post heating in air at 550 °C (a) x = 0.2 (b) x = 0.4 (c) x = 0.6 (d) x = 0.8.

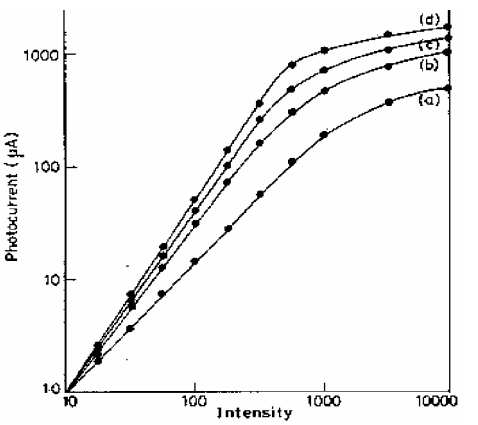

Fig. 9 Variation of photocurrent with intensity for CdS_xSe_{1-x} films of different composition deposited at 300 °C (a) x = 0.2 (b) x = 0.4 (c) x = 0.6 (d) x = 0.8.

The spectral distribution of sensitivity of the cells of different composition is shown in figure 10. Pure cadmium sulphide crystals have a peak response at 520 nm, while pure CdSe has a peak response at 720 nm [18]. This response is essentially caused by intrinsic excitation. Lattice defects that may be present in the crystal, introduces levels in the forbidden gap that require less energy than excitation across the band gap. Consequently, in crystals with such defects, the peak response may also be attributed to the presence of incorporated impurities like chloride or copper or the combined effects of copper and chloride centers [19]. Further, there is a tendency for sintered layers to have more response in the red and infrared due to copper to chloride ion ratio being more at the surface than in the bulk [20]. This may arise due to higher ratio of copper to chloride type centers at the surface of the sintered layer, than in the bulk, owing to the lower chloride concentration existing at the surface. Accompanying this increase is the relative number of copper type centers with respect to chloride type centers, there will be a deepening in the body colour of the surface. This body colour shift results in a more efficient absorption of longer wavelength, which combined with the greater effectiveness of activation due to higher copper center concentration.

The darkening of the body colour associated with increasing copper concentration at the surface primarily may introduce the possibility of affecting the position of the spectral response peak by a simple filtering action,

which is modifying the composition of the activating radiation reaching the portion of the layer involved in photoconduction. The presence of chemisorbed oxygen, on the sintered layers in particular, which act as an acceptor may also contribute to such shifts [21].

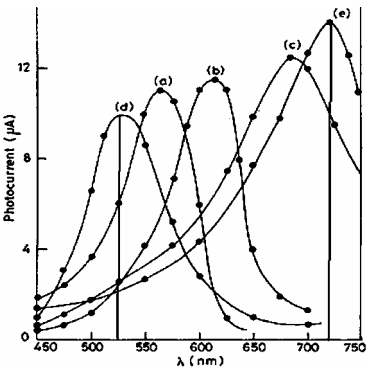

Fig. 10 Action spectra for CdS_xSe_{1-x} films of different composition deposited at 300 °C (a) x = 0.2 (b) x = 0.4 (c) x = 0.6 (d) x = 0.8 (e) x = 0.0.

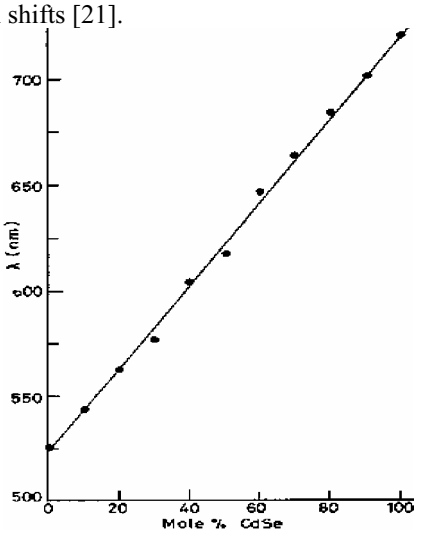

Fig. 11 Plot of wavelength of peak response with composition.

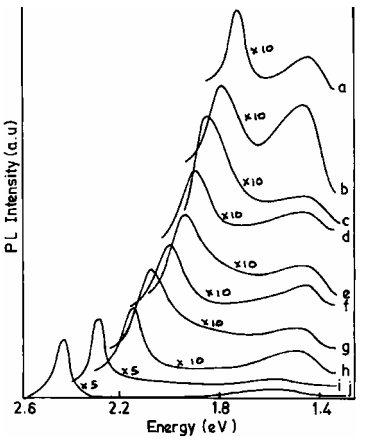

Fig. 12 Photoluminescene spectra of CdS_xSe_{1-x} films of different composition deposited at a substrate temperature of 300 °C (a) x = 0.1 (b) x = 0.2 (c) x = 0.3 (d) x = 0.4 (e) x = 0.5 (f) x = 0.6 (g) x = 0.7 (h) x = 0.8 (i) x = 0.9 (j) x = 1.0.

It is clear from the graphs that the wavelength of peak response as also the edge gets progressively shifted to longer wavelengths as the selenide content is increased. Figure 11 gives a plot of the wavelengths of peak response with composition of the CdS_xSe_{1-x} photoconductive cells. The linear increase in the wavelength of peak response is due to the solid solution formation with progressively increasing cadmium selenide content. Similar observations have been reported earlier [22].

Figure 12 shows the PL spectra of the CdS_xSe_{1-x} films at room temperature. The PL spectrum of each sample is characterized by two different radiative bands: the high energy band is related to near band edge (NBE) recombination and the low energy feature is connected to deep level transitions. The PL spectrum shifts towards lower energies with decreasing x, due to the decrease of the fundamental gap with Se composition. The large line width of the high energy band suggests that it is not due to exciton recombination, as also confirmed by its spectral position, for example, the NBE band in the CdS at 2.454 eV is at lower energy with respect to the free exciton energy reported in the literature (2.473 eV [23]). Therefore, the PL band at high energy may be assigned to transitions involving native impurity levels, such as free to bound or donor acceptor recombination. The quenching of the intensity of the NBE band in the mixed samples CdS_xSe_{1-x} with respect to CdS and CdSe is due to the larger non radiative centers introduced by means of the structural disorder of the alloys. In particular, the PL intensity of the low energy band can be considered as an indication of the defect density and structural disorder introduced in the film during the growth process: i.e. the higher the PL intensity of the low energy band with respect to the NBE band, the higher the structural disorder. Indeed, the samples characterized by the larger alloy disorder, samples with x values less than 0.7, show a broad low energy band (near 1.5 eV) that is dominant with respect to the NBE emission. Similar behaviour has been observed for pulse laser deposited films [24].

4 Conclusions

CdS_xSe_{1-x} powders of different composition ($0 < x < 1$) were successfully synthesized by a simple chemical process. Using these powders films of different composition were deposited by the electron beam evaporation technique. The band gap of the films varied from 1.68 to 2.41 eV as the concentration of CdS increased. The

root-mean-roughness (RMS) values are 3.4, 2.6, 1.2 and 0.6 nm when the composition of the films shifted towards CdS side. The films exhibited photosensitivity. The conductivity of the films changed from 30 to 480 Ωcm^{-1} with increase of CdS concentration.

References

[1] Y. Gu, E. S. Kwak, J. L. Lensch, J. E. Aller, T. W. Odom, and L. J. Lauhon, Appl. Phys. Lett. **87**, 043111 (2005).
[2] P. K. C. Pillai, N. Shroff, and A. K. Tripathi, J. Phys. D **16**, 393 (1983).
[3] A. Pan, H. Yang, R. Yu, and B. Zou, Nanotechnology **17**, 1083 (2006).
[4] A. L. Pan, H. Yang, R. B. Liu, R. C. Yu, B. S. Zou, and Z. L. Wang, J. Am. Chem. Soc. **127**, 15692 (2005).
[5] Y. Q. Liang, L. Zhai, X. S. Zhao, and D. S. Xu, J. Phys. Chem. B **109**, 7120 (2005).
[6] C. H. Ku, H. H. Chiang, and J. J. Wu, Chem. Phys. Lett. **404**, 132 (2005).
[7] L. Chen, H. Falk, P. J. Klar, W. Heimbrodt, F. Brieler, M. Froba, H. A. Krug von Nidda, A. Loidl, Z. Chen, and Y. Oka, Phys. Statuus Solidi B **229**, 31 (2002).
[8] Y. J. Hsu, S. Y. Lu, and Y. F. Lin, Adv. Funct. Mater **15**, 1350 (2005).
[9] N. Ohshima, I. Yamashita, and S. Sakimuchi, J. Inst. Telev. Eng. **30**, 976 (1976).
[10] H. Leweranz, An Introduction to luminescence of solids (Wiley, NY, 1950), p. 93.
[11] R. H. Bube, J. Appl. Phys. **32**, 1707 (1961).
[12] F. L. Chan and D. A. Brooks, Adv. X-ray Anal. **8**, 420 (1965).
[13] R. H. Bube, J. Phys. Chem. Solids **1**, 234 (1957).
[14] L. D. Budenya, I. B. Mizetskaya, and E. V. Sharkina, Tekh. Mikroelektron **23**, 539 (1976).
[15] D. P. Amalnekar, N. R. Pavaskar, S. K. Data, and A. P. B. Sinha, Ind. J. Pure. Appl. Phys. **23**, 539 (1985).
[16] P. K. Mahapatra and A. R. Dubey, Solar Energy Mater. **32**, 29 (1994).
[17] E. A. Davis and F. L. Lind, J. Phys. Chem. Solids **29**, 79 (1980).
[18] J. Woods, J. Electron. Control **3**, 225 (1957).
[19] B. Kazan and F. H. Nicoll, J. Opt. Soc. Am. **47**, 887 (1957).
[20] M. J. B. Thomas and E. J. Zdanuk, J. Electrochem. Soc. **106**, 964 (1959).
[21] H. Shear, E. A. Hilton, and R. H. Bube, J. Electrochem. Soc. **112**, 997 (1965).
[22] A. M. Pavelets, G. A. Fedorus, and M. K. Sheinkman, Ukr. Fiz. Zh. **19**,1917 (1974).
[23] R. N. Noufi, P. A. Kohl, and A. J. Bard, J. Electrochem. Soc. **125**, 375 (1978).
[24] G. Perna, S. Pagliara, V. Capozzi, M. Ambrico, and T. Ligonzo, Thin Solid Films **349**, 220 (1999).

